Mesomorphism of Hybrid Siloxane-Triphenylene Star-Shaped Oligomers

Andrés Zelcer,*,† Bertrand Donnio,*,‡ Cyril Bourgogne,‡ Fabio D. Cukiernik,†,§ and Daniel Guillon‡

INQUIMAE, Departamento de Química Inorgánica, Analítica y Química Física, Facultad de Ciencias Exactas y Naturales, Universidad de Buenos Aires, Pab. II, Ciudad Universitaria, C1428EHA Buenos Aires, Argentina, Institut de Physique et Chimie des Matériaux de Strasbourg, Groupe des Matériaux Organiques (CNRS-ULP, UMR 7504), 23 rue du Loess, BP 43, 67034 Strasbourg Cedex 2, France, and Instituto de Ciencias, Universidad Nacional de General Sarmiento, J. M. Gutierrez 1150, B1613GSX, Los Polvorines, Prov. Buenos Aires, Argentina

Received December 12, 2006. Revised Manuscript Received February 7, 2007

Novel hybrid triphenylene-carbosiloxane liquid crystalline monomers and star-shaped oligomers have been synthesized and their thermal behavior and liquid-crystalline properties analyzed and characterized. All compounds exhibit a columnar hexagonal phase and show, particularly the oligomers, a small tendency to crystallize. The substitution pattern on the central triphenylene moiety has very different effects on the crystal to columnar phase and columnar to isotropic liquid-phase transitions. A novel sterically induced superlattice has been found, and a model for the microscopic structure is proposed. One compound could be mechanically aligned, leading to well-oriented columnar liquid crystals.

Introduction

Flat, π-conjugated discotic molecules,[1] already used in phase compensation films,[2] offer a unique possibility as potential one-dimensional charge carrier systems[3] due to their ability to self-assemble into long-range 1D intermolecular columnar stackings and then into columnar organizations, preferentially the hexagonal columnar phase (Col_h). Electronic interactions as well as electrons and excitons migrations are indeed strongly favored within the columns since the stacking periodicity along the column is much shorter than the intercolumnar distance. As such, discotic liquid crystals are seen as promising organic semiconductors for applications in the domain of molecular electronics, optoelectronics, photoconductivity, photovoltaic, and electroluminescent devices.[4−9] Moreover, liquid crystals also offer many alternative advantages to organic monocrystals in that they can be more easily macroscopically aligned (monodomains) and processed, and structural defects can be self-healed because of the molecular fluctuations. However, the limited efficiency of the charge-carrier mobility (10^{-3}−0.1 $cm^2\ V^{-1}\ s^{-1}$ compared to that found in graphite of 3 $cm^2\ V^{-1}\ s^{-1}$),[10] an essential parameter to estimate for an optimal design, is in part due to the lack of long-range order of the intracolumnar stacking in the liquid-crystalline mesophase (topological defects, thermal fluctuations, and molecular diffusion). The improvement of these properties requires perfectly stable monodomains of the materials, ideally operational at ambient temperature. Various methods for increasing the extent of ordering, facilitating the processing, and improving the performances of the charge mobility have been employed. Among these, the freeze-in of the columnar order into stable, room-temperature glasses appear to be an attractive strategy since the anisotropic properties and macroscopically aligned monodomains can be easily vitrified and the ordering preserved. Triphenylene-containing liquid crystals have been the most extensively studied discotic materials for such prospects,[5,11] and examples of triphenylene-containing liquid-crystalline polymers,[12,13] elastomers,[14] networks,[15] oligomers,[13,16−18] and a wide range of symmetrically and non-symmetrically substituted monomeric

* Authors to whom correspondence should be addressed. E-mail: bdonnio@ipcms.u-strasbg.fr (B. Donnio); zelcer@qi.fcen.uba.ar (A. Zelcer).
† Universidad de Buenos Aires.
‡ Institut de Physique et Chimie des Matériaux de Strasbourg.
§ Universidad Nacional de General Sarmiento.

(1) (a) Cammidge, A. N.; Bushby, R. J. In *Handbook of Liquid Crystals*; Wiley-VCH: New York, 1998; Vol. 2B, Chapter VII, pp 693−748. (b) Kumar, S. *Chem. Soc. Rev.* **2006**, *35*, 83−109.
(2) (a) Kawata, K. *Chem. Rec.* **2002**, *2*, 59−80. (b) Okazaki, M.; Kawata, K.; Nishikawa, H.; Negoro, M. *Polym. Adv. Technol.* **2000**, *11*, 398−403.
(3) van de Craats, A. M.; Warman, J. M. *Adv. Mater.* **2001**, *13*, 130−133.
(4) Nelson, J. *Science* **2001**, *293*, 1059−1060.
(5) Boden, N.; Movaghar, B. In *Handbook of Liquid Crystals*; Wiley-VCH: New York, 1998; Vol. 2B, Chapter IX, pp 781−798.
(6) Watson, M. D.; Fechtenkötter, A.; Müllen, K. *Chem. Rev.* **2001**, *101*, 1267−1300.
(7) Bushby, R. J.; Lozman, O. R. *Curr. Opin. Solid State Mater. Sci.* **2002**, *6*, 569−578.
(8) de Halleux, V.; Calbert, J. P.; Brocorens, P.; Cornil, J.; Declercq, J. P.; Brédas, J. L.; Geerts, Y. *Adv. Funct. Mater.* **2004**, *14*, 649−659.
(9) Attias, A. J.; Cavalli, C.; Donnio, B.; Guillon, D.; Happiot, P.; Malthête, J. *Chem. Mater.* **2002**, *14*, 375−384.
(10) van de Craats, A. M.; Warman, J. M.; Müllen, K.; Geerts, Y.; Brand, J. D. *Adv. Mater.* **1998**, *10*, 36−38.
(11) Bushby, R. J.; Lozman, O. R. *Curr. Opin. Colloid Interface Sci.* **2002**, *7*, 343−354.
(12) (a) Boden, N.; Bushby, R. J.; Cammidge, A. N. *J. Am. Chem. Soc.* **1995**, *117*, 924−927. (b) Wang, T.; Yan, D. H.; Zhou, E. L.; Karthaus, O.; Ringsdorf, H. *Polymer* **1998**, *39*, 4509−4513. (c) Boden, N.; Bushby, R. J.; Lu, Z. B. *Liq. Cryst.* **1998**, *25*, 47−58.
(13) Kumar, S. *Liq. Cryst.* **2005**, *32*, 1089−1113.

10.1021/cm062949b CCC: $37.00
Published on Web 03/22/2007

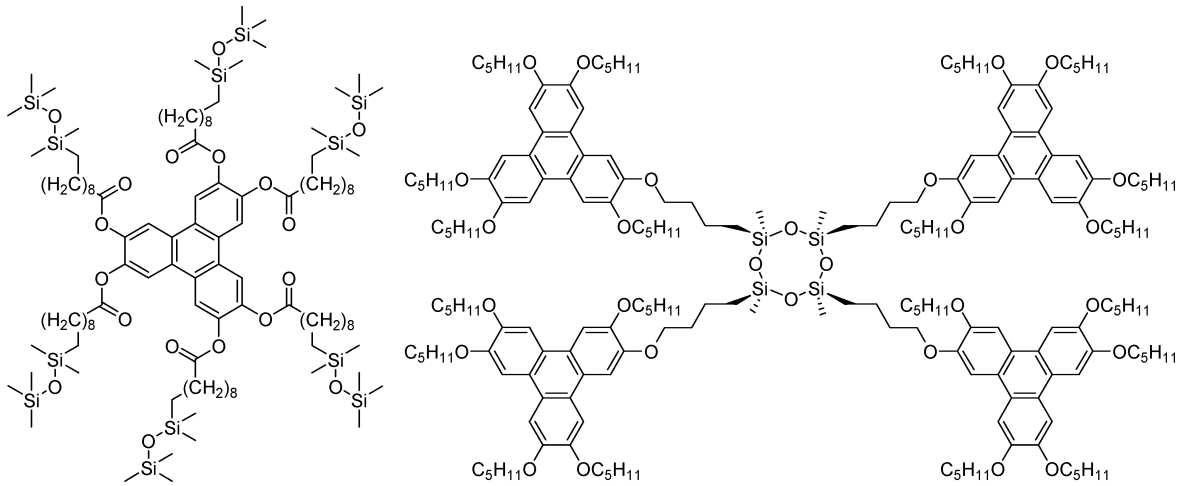

Figure 1. Previously reported low molar mass hybrid triphenylene-siloxane compounds.

systems[19] have been reported to address these points. Partially fluorinated[20] or amphiphilic[21,22] triphenylenes were also reported as structural means to enhance microsegregation.

Hybrid molecular systems that combine a siloxane part with an organic disklike group are now being considered. In general, the attachment of a flexible siloxane part to a mesogenic structure, via an alkyl spacer, maintains the liquid-crystalline property but considerably reduces the transition temperatures with respect to the aliphatic analogues. Moreover, the bulkiness of these groups disfavors crystallization and such hybrid materials show a strong tendency to freeze-in the mesophase on cooling due to a strong supercooling effect. Consequently, the mesophase temperature range becomes more accessible than their siloxane-free analogues. The triblock molecular architecture of these low-molar-mass hybrid discotic compounds consists of three chemically incompatible molecular species covalently linked together, namely, a polarizable rodlike mesogenic core, an aliphatic fragment, and the siloxane moieties. In all cases, the mesomorphism results, on the one hand, from the conflict between the preferential anisotropic order tendency of the mesogenic units and the flexibility and bulkiness of the siloxane moieties (by reducing the packing efficiency of the molecules within the mesophases) and, on the other hand, from the chemical incompatibility between the siloxane tails and the hydrocarbon mesogenic cores which will show a propensity to microsegregate in the volume, and thus enhance the mesophase stability. With respect to such an approach, a relatively small number of low-molar-mass hybrid siloxane-triphenylene discotic liquid crystals (Figure 1) have been reported and show stable columnar mesophases over a wide range of temperature, starting from room temperature.[23] Hybrid siloxane-containing liquid crystals thus form a class of potentially interesting mesogenic materials since they combine properties of mesomorphic materials with those of their poly(dimethyl)siloxane polymer analogues,[13,24] namely, the low melt viscosity of the former with the glass-forming tendency and the mechanical stability of the latter. More recently, two other promising approaches aiming at stabilizing columnar mesophases based on the stacking of triphenylene units involving dendritic architectures[25] or hydrogen-bonding supramolecular arrangements[26] are also being explored.

In this context we were interested in the design and the synthesis of new hybrid discotic oligomeric materials and in the investigation of their thermal behavior. Indeed, it is expected that these materials offer a better possibility of supramolecular ordering than their siloxane-free analogues with a good segregation between molecular moieties of

(14) (a) Bengs, H.; Finkelmann, H.; Kupfer, J.; Ringsdorf, H.; Schuhmacher, P. *Makromol. Chem., Rapid Commun.* **1993**, *14*, 445−450. (b) Disch, S.; Finkelmann, H.; Ringsdorf, H.; Schuhmacher, P. *Macromolecules* **1995**, *28*, 2424−2428.
(15) (a) Favre-Nicolin, C. D.; Lub, J. *Macromolecules* **1996**, *29*, 6143−6149. (b) Braun, C. D.; Lub, J. *Liq. Cryst.* **1999**, *26*, 1501−1509. (c) Feng, X. S.; Pan, C. Y. *ChemPhysChem.* **2002**, *3*, 539.
(16) (a) Boden, N.; Bushby, R. J.; Cammidge, A. N.; Martin, P. S. *J. Mater. Chem.* **1995**, *5*, 1857−1860. (b) Plesnivy, T.; Ringsdorf, H.; Schuhmacher, P.; Nutz, U.; Diele, S. *Liq. Cryst.* **1995**, *18*, 185−190. (c) Boden, N.; Bushby, R. J.; Cammidge, A. N.; El-Mansoury, A.; Martin, P. S.; Lu, Z. B. *J. Mater. Chem.* **1999**, *9*, 1391−1402.
(17) Schulte, J. L.; Laschat, S.; Vill, V.; Nishikawa, E.; Finkelmann, H.; Nimtz, M. *Eur. J. Org. Chem.* **1998**, 2499−2506.
(18) Maliszewskyj, N. C.; Heiney, P. A.; Josefowiczt, J. Y.; Plesnivy, T.; Ringsdorf, H.; Schuhmacher, P. *Langmuir* **1995**, *11*, 1666−1674.
(19) (a) Cross, S. J.; Goodby, J. W.; Hall, A. W.; Hird, M.; Kelly, S. M.; Toyne, K. J.; Wu, C. *Liq. Cryst.* **1998**, *25*, 1−11. (b) Allen, M. T.; Harris, K. D. M.; Kariuki, B. M.; Kumari, N.; Preece, J. A.; Diele, S.; Lose, D.; Hegmann, T.; Tschierske, C. *Liq. Cryst.* **2000**, *27*, 689−692. (c) Allen, M. T.; Diele, S.; Harris, K. D. M.; Hegmann, T.; Kariuki, B. M.; Lose, D.; Preece, J. A.; Tschierske, C. *J. Mater. Chem.* **2001**, *11*, 302−311. (d) Kumar, S. *Liq. Cryst.* **2004**, *31*, 1037−1059.
(20) (a) Dahn, U.; Erdelen, C.; Ringsdorf, H.; Festag, R.; Wendorff, J. H.; Heiney, P. A.; Maliszewskyj, N. C. *Liq. Cryst.* **1995**, *19*, 759−764. (b) Terasawa, N.; Monobe, H.; Shimizu, Y. *Chem. Lett.* **2003**, *32*, 214−215.
(21) Boden, N.; Bushby, R. J.; Jesudason, M. V.; Sheldrick, B. *J. Chem. Soc., Chem. Commun.* **1988**, 1342−1343.
(22) Barberá, J.; Garcés, A. C.; Jayaraman, N.; Omenat, A.; Serrano, J. L.; Stoddart, J. F. *Adv. Mater.* **2001**, *13*, 175.
(23) (a) Kumar, S.; Schuhmacher, P.; Henderson, P.; Rego, J.; Ringsdorf, H. *Mol. Cryst. Liq. Cryst.* **1996**, *288*, 211−222. (b) Haarer, D.; Simmerer, J.; Schuhmacher, P.; Paulus, W.; Etzbach, K. H.; Siemensmeyer, K.; Ringsdorf, H. *Mol. Cryst. Liq. Cryst.* **1996**, *283*, 63−68. (c) Markovitsi, D.; Marguet, S.; Bondkowski, J.; Kumar, S. *J. Phys. Chem. B* **2001**, *105*, 1299−1306. (d) Zniber, R.; Achour, R.; Cherkaoui, M. Z.; Donnio, B.; Gehringer, L.; Guillon, D. *J. Mater. Chem.* **2002**, *12*, 2208−2213.
(24) Finkelmann, H. In *Thermotropic Liquid Crystals*; Gray, G. W., Ed.; John Wiley & Sons: New York, 1987; Vol. 22.
(25) McKenna, M. D.; Barbera, J.; Marcos, M.; Serrano, J. L. *J. Am. Chem. Soc.* **2005**, *127*, 619−625.
(26) Paraschiv, I.; Giesbers, M.; van Lagen, B.; Grozema, F. C.; Abellon, R. D.; Siebbeles, L. D. A.; Marcelis, A. T. M.; Zuilhof, H.; Sudholter, E. J. R. *Chem. Mater.* **2006**, *18*, 968−974.

Chart 1. Schematic Representation of the Cross-Coupling Reactions Plan Starting from HAT*n* for the Preparation of the Hybrid Triphenylene Materials

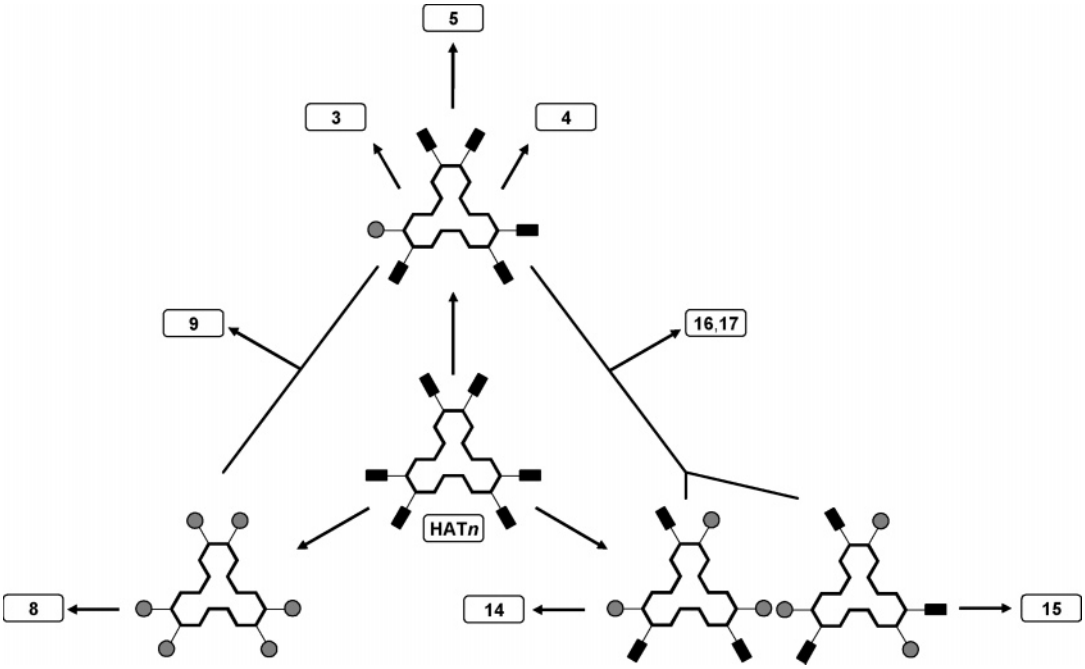

different natures, and moreover the ordering is not constrained by the presence of a long polymeric backbone. We report herein the synthesis and the liquid-crystalline properties of hexa(alkoxy)-substituted triphenylenes containing either terminal double bonds (the precursors) or terminal disiloxane groups, as model compounds, including mono-, tri-, and hexafunctionalized derivatives. To obtain stabilized columnar mesophases where lateral slippage of molecules from one column to the adjacent one is strongly prevented, larger oligomeric molecules including a disiloxane-bridged dimer (**5**), two starlike tetramers isomers (**16** and **17**), and a starlike heptamer (**9**) were prepared and studied.

Results

Methodology. To synthesize these various triphenylene-based oligomers, it was necessary to optimize the synthesis of the intermediates and to limit the number of precursors. Thus, instead of long and tedious multistage synthesis procedures involving successive elementary protection steps, selective coupling procedures,[27] and low-yields deprotection reactions, the statistical mono- and tris-dealkylation of hexakis(hexyloxy)triphenylene (**HAT6**) with bromocatecholborane was preferred.[28] As such, the monohydroxy **1**, the C_3 trihydroxy derivative **11** and its nonsymmetrical isomer **10**, precursors of the dimer **5** and heptamer **9**, and both tetramers **17** and **16**, respectively, were easily obtained. This approach only necessitates the preparation of a symmetrical triphenylene precursor (**HAT*n***), by oxidative trimerization of the appropriate dialkoxybenzene, as the main building brick for all these hybrid triphenylenes (Chart 1). The proportion and nature of the hydroxyl derivatives in the mixture resulting from this statistical cleavage procedure can be controlled by the experimental conditions. Thus, the hydroxyl **1** is obtained in about 70% yields when 1.1−1.2 equiv of catecholborane per **HAT*n*** is used, whereas if 3.6 equiv of the borane is used, an approximate 3:2 mixture of both trishydroxyl isomers (**11**:**10**) is obtained, which can be separated by chromatography techniques.[28,29] As for the heptamer **9**, its synthesis also relied upon the total demethylation of hexakis(methoxy)triphenylene (**HAT1**) in HBr/HOAc to yield the corresponding hexahydroxtriphenylene. These various hydroxy derivatives were further modified by alkylation to form the intermediate olefinic compounds **2**, **12**, **13**, and **7**.

Synthesis. Hexakis(hexyloxy)triphenylene (**HAT6**) was synthesized using $FeCl_3$ oxidative coupling of dihexyloxybenzene in dichloromethane (Scheme 1).[30] It was partially dealkylated using B-bromocathecholborane[28] to yield the monofunctional hydroxy derivative **1** (Scheme 1). Reaction of this hydroxy derivative with 5-bromo-pent-1-ene under typical Williamson's etherification conditions yielded the corresponding mixed alkene-pentaalkyl triphenylene **2**. Hydrosilylation of **2** with an excess of pentamethyldisiloxane (PMDS) or tetramethyldisiloxane (TMDS) yielded the siloxane derivatives **3** and the key silane hybrid precursor **4**—the crucial intermediate for the preparation of the oligomers **9**, **16**, and **17**—respectively. The dimer **5** was produced by reacting 1 equiv of **2** with 0.5 equiv of TMDS; the moderate yield of the reaction was likely due to the volatility of TMDS.

The hexahydroxytriphenylene **6** was obtained from hexamethoxytriphenylene (**HAT1**) by complete demethylation

(27) Pérez, D.; Guitián, E. *Chem. Soc. Rev.* **2004**, *33*, 274−283.
(28) Kumar, S.; Manickam, M. *Synthesis* **1998**, 1119−1122.
(29) Manickam, M.; Belloni, M.; Kumar, S.; Varshney, S. K.; Shankar Rao, D. S.; Ashton, P. R.; Preece, J. A.; Spencer, N. *J. Mater. Chem.* **2001**, *11*, 2790−2800.
(30) (a) Boden, N.; Borner, R. C.; Bushby, R. J.; Cammidge, A. N.; Jesudason, M. V. *Liq. Cryst.* **1993**, *15*, 851−858. (b) Boden, N.; Bushby, R. J.; Cammidge, A. N. *J. Chem. Soc., Chem. Commun.* **1994**, 465−466.

Scheme 1. Synthesis of the Hybrids 3, 4, and 5 and of Their Precursory Monomeric Intermediates

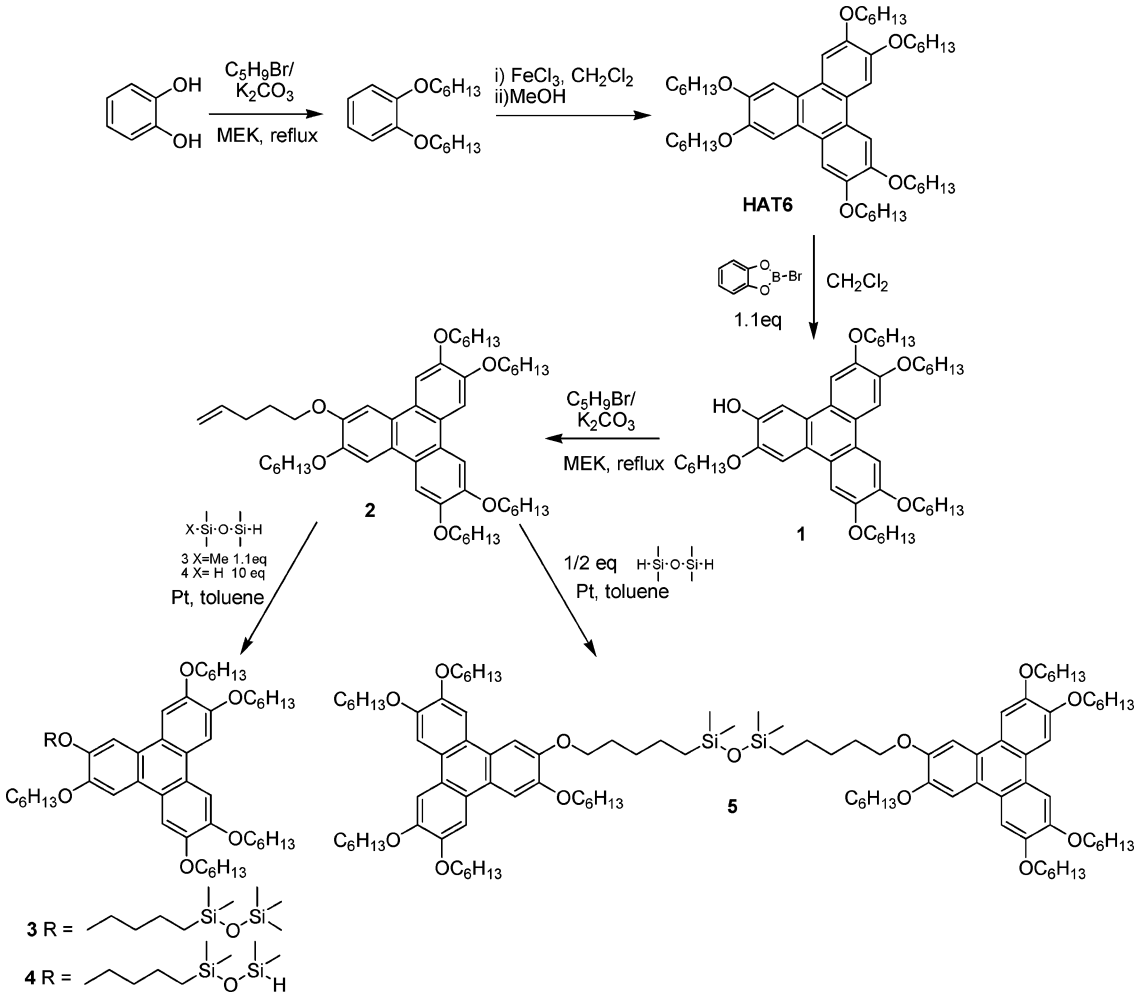

using either HBr[31] or BBr_3[32] (Scheme 2). Reaction with 5-bromo-pent-1-ene yielded the hexafunctional alkene core **7**. Hydrosilylation of this alkene with either pentamethyldisiloxane or with the triphenylene-silane hybrid **4** gave compound **8** and the heptamer **9**, respectively.

To achieve the synthesis of the other mixed alkyl-alkene triphenylenes **12** and **13**, the same strategy was followed implicating the partial dealkylation of **HAT6** and then the trialkylation with bromopentene. The statistical cleavage of the hexyl chains of **HAT6** with bromocathecholborane[28] yielded the two desired trifunctional hydroxy isomers, namely, **10** (*unsymmetrical*) and **11** (*symmetrical*), that could be separated by chromatography on silica (Scheme 3). Reaction of these hydroxy derivatives with 5-bromo-pent-1-ene yielded the two corresponding trifunctional isomeric alkenes **12** (*unsymmetrical*) and **13** (*symmetrical*). Then, hydrosilylation of these alkenes with pentamethyldisiloxane afforded the corresponding disiloxane terminated derivatives (**14** and **15**). The synthesis of the tetrameric starlike compounds **16** and **17** was achieved by hydrosilylation of the same alkenes with the reactive triphenylene-silane hybrid **4** (Scheme 3).

Characterization. The structure and analytical purity of the synthesized compounds were confirmed by TLC, ^{1}H NMR, ^{13}C NMR, and elemental analysis. DEPT, GPC, and mass spectra (EI, FAB, or MALDI) experiments were also carried out for some specific cases.

The essential features of NMR spectra are typical of substituted triphenylenes and consistent with the proposed structures. Integrations protons ratio (^{1}H NMR) is the feature that permits one to distinguish each compound, especially the relationships between the terminal methyl groups, CH_3, at 0.93 ppm, the methylene groups linked to the silicon atom, CH_2Si, at 0.59 ppm, and the aromatic protons (at $\sim$ 7.80 ppm). The main data are given in the Experimental Section for each compound, as well as the elemental analysis.

Mass spectrometry also appeared a very useful technique to confirm the structure of the synthesized compounds and was essential in the characterization of heptamer **9**. Indeed, molecular mass and isotopic distributions on $M^{+\bullet}$ agreed with the expected ones for **8** (m/z = 1620.6), **9** (m/z = 6418.2), **14** and **15** (m/z = 1224.7), and **16** and **17** (m/z = 3620.5), as did molecular mass and fragmentations in the case of **4** (m/z = 946.6). In addition to the expected $[M]^{+\cdot}$ signal, MALDI-TOF in the case of compounds **9**, **16**, and **17** and also EI in the case of **4** revealed the presence of molecules of slightly higher m/z than the expected molecular ion (m/z = 1020.6 for **4**, m/z = 6493.2 for **9**, and m/z = 3694.6 for

(31) Krebs, F. C.; Schiodt, N. C.; Batsberg, W.; Bechgaard, K. *Synthesis* **1997**, 1285−1290.
(32) McOmie, F. W.; Watts, M. L.; West, D. E. *Tetrahedron* **1968**, *24*, 2289−2292.

Scheme 2. Synthesis of the Hybrids 8 and 9 and of Their Precursory Monomeric Intermediates

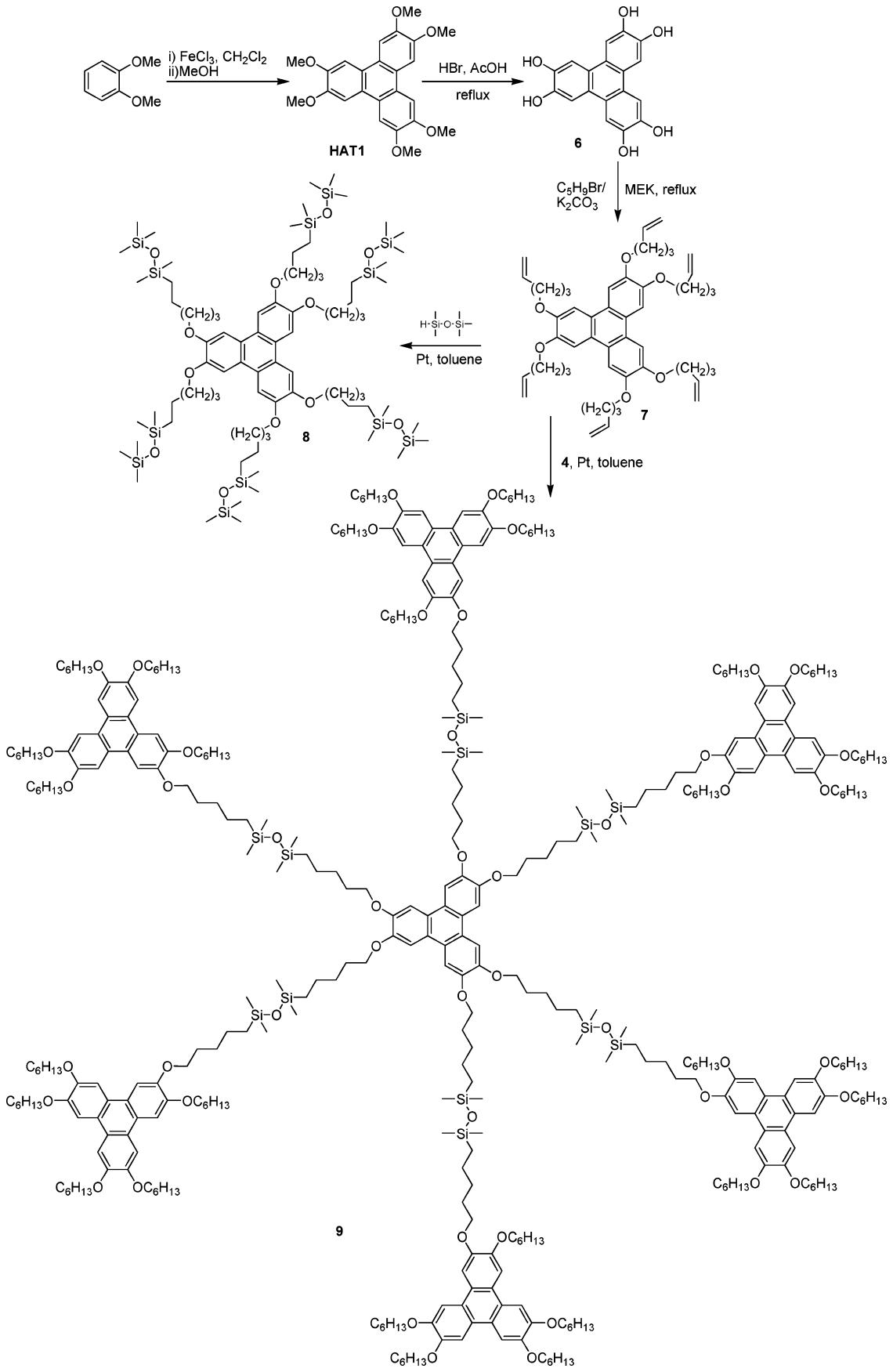

16 and **17**). This *m*/*z* difference corresponds well to an extra dimethylsiloxane unit, $[M + Si(CH_3)_2O]^{+\bullet}$. This extra dimethylsiloxane group was likely introduced during the synthesis of **4**, due to the presence of hexamethyltrisiloxane instead of tetramethyldisiloxane as terminal substituents. Indeed, GC analysis of commercial tetramethyldisiloxane

Scheme 3. Synthesis of the Hybrids 14, 15, 16, and 17 and of Their Precursory Monomeric Intermediates

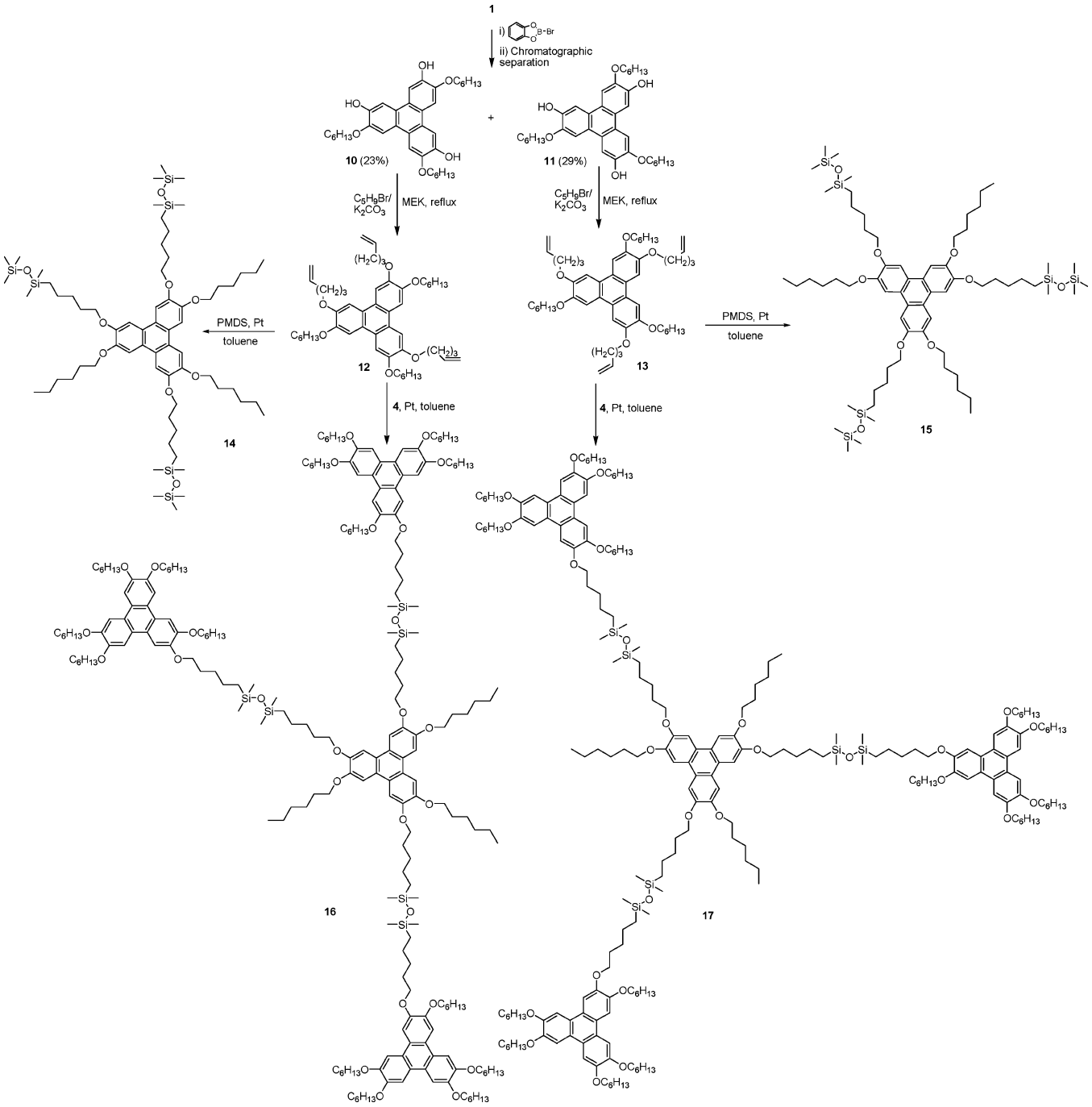

confirmed the presence of traces of hexamethyldisiloxane (ca. 3%); thus, a binomial distribution of products with an extra $Si(Me)_2O$ group is expected, as is approximately found in the MALDI-TOF spectrum of **9**.

Thermal and Mesomorphic Behavior. The thermal and mesomorphic behavior of all new compounds was studied by polarized optical microscopy (POM), thermogravimetric analysis (TGA), differential scanning calorimetry (DSC), and variable temperature X-ray diffraction (XRD). The transition temperatures, phase sequence, and thermodynamic data are collected in Table 1.

All the compounds have a good thermal stability as TGA showed decomposition only above 200 °C, well above the isotropization temperature. Even so, for the alkene-substituted triphenylenes, the initial decomposition pathway could be due to addition reaction or polymerization between double bonds, so loss of mass is not expected. Nevertheless, reproducibility between DSC cycles proved that no decomposition occurred in the isotropic liquid near the clearing temperatures.

POM. When observed under POM, all the studied compounds exhibited fluid and homogeneous textures characteristic of columnar mesophases, as shown for example in Figure 2 for a representative selection of materials. The transition temperatures measured by DSC and POM experiments agreed within experimental errors. On cooling from the isotropic liquid, homeotropic uniaxial and large cylindrical domains were observed for most optical texture samples, and occasionally dendritic growth of the columnar phase from the isotropic phase was seen. None of the siloxane-

Table 1. Thermal Behavior and X-ray Characterization

compds	mesomorphism and phase sequence[a] transition temperatures (°C) transition enthalpies ($kJmol^{-1}$)	X-ray diffraction[b] T (°C)	$d_{exp.}$ (Å)	hk	I	d_{calc} (Å)	mesophase parameters[c]
2	Cr 56.9(37.9) Col_h 99.2(5.7) I	60	18.11 4.47 3.57	10	VS Br (CH_2) Sh ($\pi-\pi$)	–	$a = 20.9$ Å $S = 379$ Å^2 $V = 1350$ Å^3 $h = 3.56$ ($N = 1$)
3	Cr 43.0(41.2) Col_h 76.4(2.7) I	60	19.88 11.47 4.6 3.6	10 11	VS M Br (CH_2) Sh ($\pi-\pi$)	19.88 11.48	$a = 22.9$ Å $S = 456$ Å^2 $V = 1600$ Å^3 $h = 3.5$ ($N = 1$)
4	Cr 41.6(41.2) Col_h 74.5(2.8) I	60	19.75 11.40 4.6 3.6	10 11	VS M Br (CH_2) Sh ($\pi-\pi$)	19.75 11.40	$a = 22.8$ Å $S = 450$ Å^2 $V = 1570$ Å^3 $h = 3.5$ ($N = 1$)
5	Cr 45.6(81) Col_h 88(9.6) I	70	19.04 10.96 4.5 3.6	10 11	VS M Br (CH_2) Sh ($\pi-\pi$)	19.01 10.98	$a = 21.9$ Å $S = 417$ Å^2 $V = 2925$ Å^3 $h = 3.51$ ($N = 1/2$)
7	Cr 78.3(33.3) Col_h 97.1(4.3) I	85	16.67 4.5 3.7	10	VS Br (CH_2) Sh ($\pi-\pi$)	–	$a = 19.2$ Å $S = 321$ Å^2 $V = 1215$ Å^3 $h = 3.8$ ($N = 1$)
8	Cr −19 Col_h 52.6(5.3) I [G −76.1]	20	23.44 13.58 11.76 8.85 6.3 4.2	10 11 20 21	VS M M M Br ($SiMe_2O$) Br (CH_2)	23.48 13.56 11.74 8.87	$a = 27.1$ Å $S = 637$ Å^2 $V = 2695$ Å^3 $h = 4.23$ ($N = 1$)
9	PCr 38 Col_h 111.0(35.5) I	80	38.9 19.26 11.10 9.62 4.6 3.6	1/2 10 11 20	W VS M M Br (CH_2) Sh ($\pi-\pi$)	38.5 19.24 11.11 9.62	$a = 22.2$ Å $S = 428$ Å^2 $V = 10655$ Å^3 $h = 3.56$ ($N = 1/7$)
12	Cr 47.7(37.3) Col_h 96.4(4.8) I	55	17.63 4.3 3.6	10	VS Br (CH_2) Sh ($\pi-\pi$)	–	$a = 20.4$ Å $S = 359$ Å^2 $V = 1300$ Å^3 $h = 3.62$ ($N = 1$)
13	Cr 64.8(39.6) Col_h 95.8(4.8) I	75	17.6 4.5 3.6	10	VS Br (CH_2) Sh ($\pi-\pi$)	–	$a = 20.3$ Å $S = 357$ Å^2 $V = 1300$ Å^3 $h = 3.64$ ($N = 1$)
14	Cr 2.5(32.3) Col_h 83.3(5.5) I	30	22.64 13.07 11.30 6.2 4.6 3.6	10 11 20	VS M M Br ($SiMe_2O$) Br (CH_2) Br, w ($\pi-\pi$)	22.63 13.07 11.32	$a = 26.13$ Å $S = 592$ Å^2 $V = 2040$ Å^3 $h = 3.46$ ($N = 1$)
15	PCr 31.2 Col_h 86.0(5.8) I [G −64.3]	40	22.72 13.18 11.37 6.3 4.6 3.6	10 11 20	VS M M Br ($SiMe_2O$) Br (CH_2) Sh ($\pi-\pi$)	22.76 13.14 11.38	$a = 26.3$ Å $S = 598$ Å^2 $V = 2040$ Å^3 $h = 3.42$ ($N = 1$)
16	PCr 30.5 Col_h 108.05(23.3) I [G −44.9]	60	19.29 11.15 4.5 3.5	10 11	VS M Br (CH_2) Sh ($\pi-\pi$)	19.30 11.14	$a = 22.3$ Å $S = 430$ Å $V = 6020$ Å^3 $h = 3.5$ ($N = 1/4$)
17	Am 54.1 Col_h 106.1(20.5) I [G −43.2]	80	19.32 11.14 4.6 3.6	10 11	VS M Br (CH_2) Sh ($\pi-\pi$)	19.31 11.15	$a = 22.3$ Å $S = 431$ Å $V = 6020$ Å^3 $h = 3.5$ ($N = 1/4$)

[a] G = glass, Cr = crystal, Col_h = columnar hexagonal phase, I = isotropic liquid, Am = amorphous, PCr = partially crystalline solid. Glass transitions correspond to the second heating. [b] T is the temperature of the XRD experiment, and $d_{exp.}$ and $d_{calc.}$ are the experimentally measured and calculated diffraction spacings at T. The distances are given in Å, hk is the indexation of the reflections. Intensity of the reflections: VS, very strong; S, strong; M, medium; W, weak; VW, very weak; Br and Sh stand for broad and sharp (diffuse) reflections, respectively. $d_{calc.}$ is deduced from the following mathematical expressions: $\langle d_{10}\rangle = 1/N_{hk}[\Sigma_{hk} d_{hk}.(h^2 + k^2 + hk)^{1/2}]$ where N_{hk} is the number of hk reflections observed. [c] The lattice parameter, a, is defined as $a = 2\langle d_{10}\rangle/\sqrt{3}$ and the lattice area, S, is $S = a^2\sqrt{3}/2$. V is the molecular volume and was calculated considering a density of 1 according to $V = MW/0.6022$, where MW is the molecular weight. h is the intracolumnar repeating distance, deduced directly from the calculated molecular volume and the measured columnar cross section according to $h = NV/S$, where N is the number or a fraction of molecules.

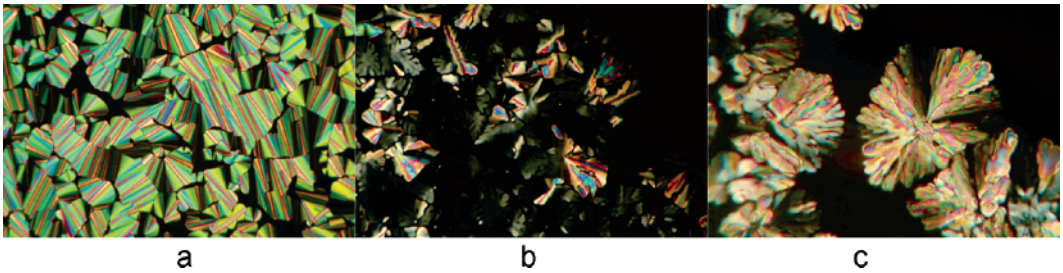

Figure 2. Typical textures: observed by POM: (a) **12** at 94 °C; (b) **14** at 73 °C; (c) **9** at 113 °C. All images are taken on cooling from the isotropic liquid.

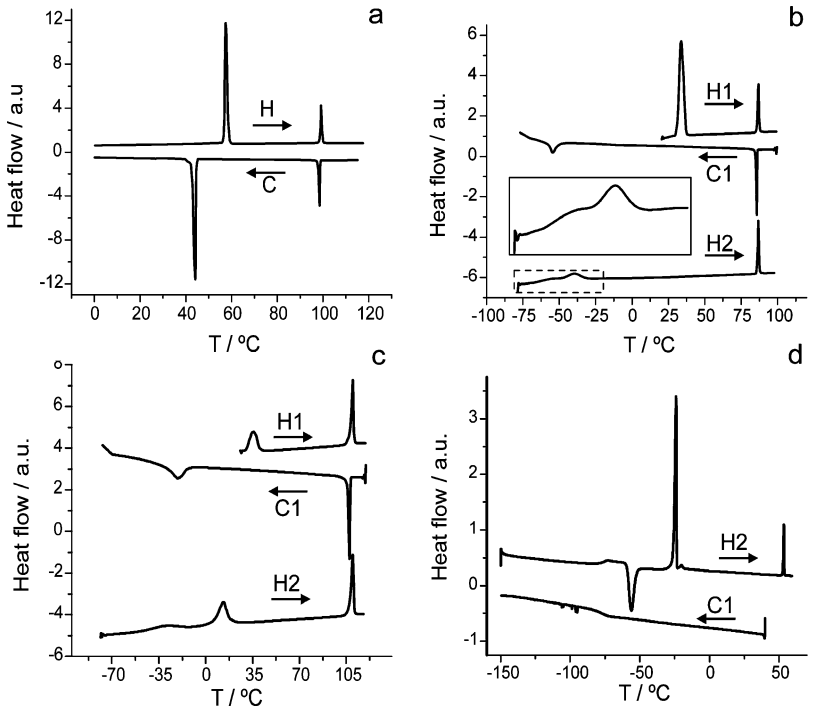

Figure 3. DSC traces of compound **2** (a), compound **15** (b), compound **16** (c), and compound **8** (d) at 5 °C/min. C and H stand for cooling and heating cycles, respectively.

containing samples showed evidence of crystallization when observed under microscope.

DSC. To study the thermodynamic parameters of the phase transitions, DSC experiments were performed at scanning rates of 5 and 2 °C/min. Very narrow phase transitions were observed for all the compounds, with perfect coincidence of clearing transition temperatures on heating and cooling. Results of these investigations are summarized in Table 1.

DSC of all olefinic compounds showed two transitions during both heating and cooling cycles, corresponding to crystal to columnar and columnar to isotropic phase transitions. On cooling, while the isotropic to columnar phases transition temperature was perfectly coincident with that of the heating run, the columnar to crystalline phase transition showed an important supercooling effect (see Figure 3a).

The behavior of the siloxane-containing compounds is quite different: all but **8** showed signs of a crystal to columnar phase transition during the first heating run, but only **3**, **4**, **5**, and **14** crystallized during the cooling cycle. On cooling, **8** showed only a glass transition at −73 °C, also visible on the subsequent heating (see Figure 3d). In contrast, an exothermic transition corresponding to a cold crystallization took place while heating the sample (−59 °C at 2 °C/min). The other siloxane-containing compounds (**9**, **15**, **16**, and **17**) showed a transition on cooling, presumably corresponding to the transformation of the supercooled columnar phase into a glassy phase, or a to a partial crystallization concomitant to a glass transition. Subsequent heating results in a glass transition and the transformation to the liquid-crystalline phase, without crystallization (see Figures 3b and 3c). This transformation occurs in one single step in the case of **15** and **16** or in a series of transitions in the case of **9** and **17**. During the first run most of the siloxane-containing compounds were only partially crystalline, consecutive to slow crystallization kinetics, so that the latent heat corresponding to the crystal to columnar phase transition could not be determined accurately. In fact, siloxane-bridged oligomers (dimer **5**, heptamer **9**, and tetramers **16** and **17**) crystallize very slowly at room temperature. DSC experiments showed that **5** was found to crystallize in the time scale of months and **9** was only ∼50% crystalline after 1 year at room temperature.

Small-Angle X-ray Diffraction. The nature and structural characteristics of the mesophases were determined by small-angle X-ray diffraction (XRD) as a function of temperature and the results are summarized in Table 1.

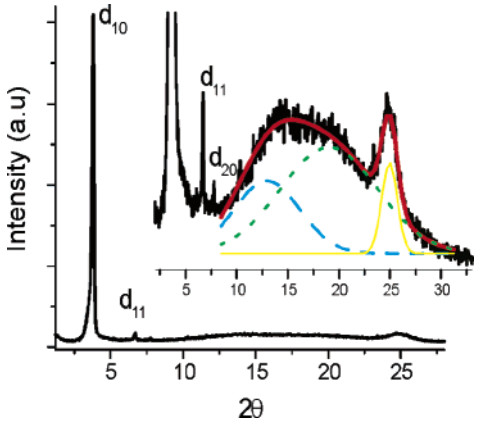

Figure 4. X-ray diffraction pattern of compound **15** recorded at 50 °C. The deconvolution curve shows the characteristic distances of the $\pi-\pi$ stacking (yellow), molten aliphatic chains (green), and siloxane groups (blue).

XRD patterns obtained for all siloxane-containing molecules exhibited at least two main signals in the reciprocal spacing ratio 1:$\sqrt{3}$, confirming the arrangement of the columns into a hexagonal lattice (see Figure 4 and Table 1). The columnar structure of olefinic compounds **2**, **7**, **12**, and **13** do not seem as well-developed, as the XRD patterns exhibited only one single sharp and intense signal in the small angles, corresponding to the fundamental reflection. Based on the POM experiments, and on the general behavior of triphenylene liquid-crystal materials,[1,13] the mesophases were nevertheless assigned as hexagonal columnar phases and analyzed accordingly.

In addition, the XRD patterns also exhibited a broad signal at ca. 4.5 Å for all studied compounds, indicative of the liquid-like ordering of the molten aliphatic chains portions. Another rather sharp signal at ca. 3.6 Å, assigned to the intracolumnar π stacking of the triphenylene cores, was observed for all compounds but **8**; it is broad for **14**. Another broad peak at 6.3 Å, assigned to the molten siloxane moieties, was observed for only three monomeric siloxane-containing compounds, namely, **8**, **14**, and **15** (for **14** and **15**, interdigitation of siloxane segments from neighboring molecules is inevitable), but it was absent in **3** and **4** and in the oligomeric series, i.e., **5**, **9**, **16**, and **17** (see Table 1).

In the case of **8**, four peaks in the reciprocal ratio 1:$\sqrt{3}$:$\sqrt{4}$:$\sqrt{7}$ were detected, indexed as the 10, 11, 20, and 21 reflections of the hexagonal *p*6*mm* 2D lattice group. This is the only compound for which no signal at 3.6 Å was found, likely due to the steric hindrance of the bulky siloxane terminal groups which do not permit a regular close stacking of the mesogens along the columnar axis. Finally, an additional weak but sharp peak was observed in the small-angle part (around 40 Å[33]) of the XRD patterns of heptamer **9** (Figure 5). This reflection was assigned to a superlattice induced by steric repulsion between siloxanes moieties (see Discussion).

Mechanical Alignment. Intensities of XRD reflections corresponding to the hexagonal lattice of compound **16** before and after heating through the clearing point were very different. As we used a 1D curved gas counter as a detector, this suggested that the sample was aligned when the first set of diffraction patterns was registered. To prove if the capillary filling process aligned the sample, we performed XRD experiments using a punctual beam and a 2D detector. The sample was rolled between two glass slides, adopting a cylindrical shape. The diffraction pattern thus obtained was highly anisotropic, showing two halos at 3.6 Å ($\pi-\pi$ stacking) rotated 90° from two spots at 19.3 Å (the 10 reflection, see Figure 6).

(33) This signal was observed in three different diffractometers, at cathode potentials low enough to preclude an artifact due to *bremsstrahlung*.

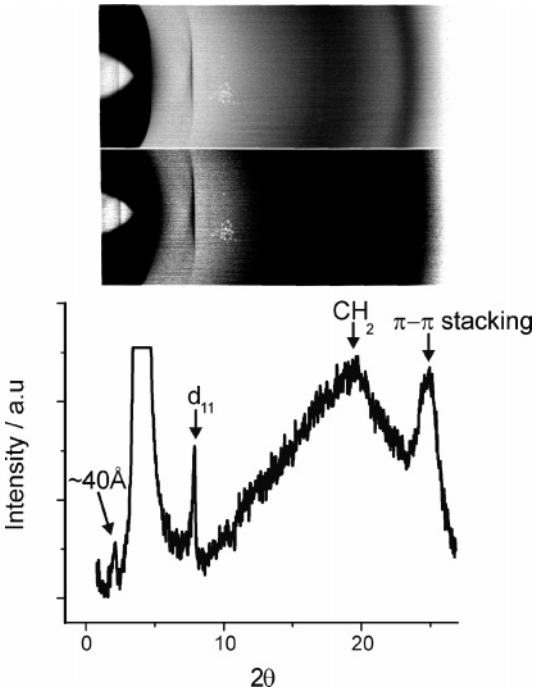

Figure 5. Image plate and intensity profile of the Col_h phase of compound **9** registered at 80 °C.

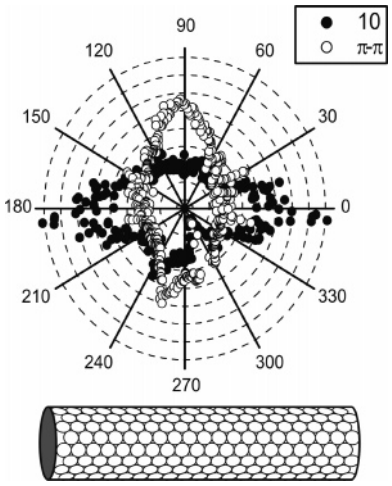

Figure 6. Normalized angular diffraction intensity of aligned **16** at the 10 and $\pi-\pi$ stacking distances. The cylinder orientation shows the disposition of the sample relative to the detector. The small circles represent the columns sections inside of the sample.

Discussion

As deduced from POM and XRD experiments, all the studied compounds showed a discotic columnar hexagonal phase with transition temperatures close to those already found in related systems.[1,13] The presence of a signal at ca.

3.6 Å for all compounds but **8** proves that there is quasi-long-range intracolumnar stacking order along the columns. The synthetic route chosen proved to be versatile and allowed us to prepare new hybrids and oligomers, including a constitutional isomeric pair, thus taking advantage of the richness of substitution possibilities on triphenylene.

Thermal Behavior. Although substitution with terminal alkene chains usually depresses the melting temperatures,[23d,34] **7** has a higher melting temperature than its saturated hexakis-(pentyloxy)triphenylene homologue (Cr 69 Col 122 I[35]). Additional interactions brought by the double bonds and the efficiency of the solid-state molecular packing, dependent on the molecular shape, are likely to be responsible for the enhanced crystal phase stability. The depression of the clearing that points up to 25 °C with respect to the fully saturated homologue strictly follows the trend already observed in compounds bearing olefinic side chains; the mesophases stability is then affected according to the sequence **2** → **12** → **7**,[19b,c,36] following the increase in the number of double bonds.[34]

Upon the grafting of siloxane groups, both the crystal phase and the mesophase of the hybrid systems are destabilized, with an important depression of the melting transition temperatures, whereas the reduction of the clearing temperatures is lesser. This observation remains valid for all the pairs of olefinic-siloxane derivatives (**2** → **3**, **7** → **8**, **12** → **14**, **13** → **15**). In most cases (with the exception of **3**), the mesomorphic temperature ranges were substantially increased, with room-temperature mesophases occurrence. Moreover, very little variations of the mesomorphic properties within the oligomers were detected (both tetramers and the heptamer exhibit almost identical thermal behavior), but the mesophases stabilities were greatly enhanced when compared to those of the monomeric siloxane homologues (**3** → **5**, **8** → **9**, **14** → **16**, **15** → **17**).

Comparison of the latent heat and temperature of transition of pairs of isomeric compounds (**12**−**13**, **14**−**15**, **16**−**17**) suggests that the substitution pattern on the triphenylene core seems to be of little importance for the columnar to isotropic phase transition: rotational and translational degrees of freedom of the molecules are already active and the entropic gain is similar for the isotropization of all isomers. On the other hand, thermodynamics and kinetics of transitions to and from the low-temperature solid phase are very dependent on the geometry of the molecule, possibly because the packing of each compound in the crystalline phase is very different. The most evident effect of this difference can be seen in the over 20 °C difference in the melting temperature of the pairs of compounds **12** and **13**, **16** and **17**, and **14** and **15**. In this last pair the difference is even more obvious as isomer **14** crystallizes on cooling while **15** does not.

As already seen,[16,37] the slow crystallization kinetics of oligomeric compounds "freezes" the mesophase into a glassy state, with a low-temperature glass transition. In fact, both tetramers **16** and **17**, heptamer **9**, and even monomeric compounds **8** and **15** do not crystallize when cooled at 2 °C/min. This behavior is not surprising in oligomeric materials, where molecular motions are restricted due to the mechanical attachment of the mesogens to another one, possibly in a different column, thus forming columnar networks. This constraint increases the viscosity of the system up to the glass transition, where no further molecular motion takes place. In contrast, monomeric compounds, in spite of lacking intercolumnar links, can still turn and flip to arrange in a suitable manner.[16] That compound **14** crystallizes while its constitutional isomer **15** does not, despite the lower molecular symmetry of the former, suggests that its microscopic viscosity is lower. This could be a result of having two "sides" (**14**) without bulky siloxane groups, resulting in a lower barrier for rearrangement by slipping from one column to the other. It is very likely that the way the molecules are packed in the crystalline state plays a significant role in the different thermal behaviors observed.

Mesophase Structure. The hexagonal lattice parameter *a* in the liquid-crystalline states varies from 19.2 Å for **7**, having six peripheral pentenyloxy chains, to 27.1 Å for **8**, containing the largest number of carbosiloxane fragments. The intercolumnar distance is clearly correlated with the proportion of siloxane units to methylene units, being greater for the siloxane-rich compounds. This growth seems to saturate after the proportion gets higher than that in trisubstituted compounds **14** and **15**, where the distance (26.3 Å) is very close to that of the hexasubstituted compound **8**.

The 2D hexagonal lattice is best developed for compound **8** (four small-angle Bragg reflections), the only one completely "crowned" by disiloxane units. Its mesophase can thus be described as a hexagonal arrangement of parallel columns, each column consisting of two concentric segregated cylindrical portions, an internal cylinder made of the aromatic core surrounded by the aliphatic crown, and with the interstitial region being filled by a silicon continuum (in agreement with the broad band of the molten siloxane part at 6.3 Å). To a lesser extent, the observation of the siloxane broad band in the Col_h X-ray patterns of **14** and **15** suggests a similar model of concentric rings of various natures, realized by interdigitation of the siloxane moieties between adjacent columns (in agreement with a slight decrease of the lattice parameters of the Col_h phase from 27.1 Å for **8** to 26.13−26.3 Å for **14** and **15**, concomitant with a thinner siloxane continuum).

Such kind of enhanced structural organization, promoted by diblock or triblock architecture, is common in liquid-crystalline polymers, but has also been observed in molecular systems, the most striking case being probably that of semifluorinated alkanes[38] exhibiting smectic phases. The

(34) (a) Collard, D. M.; Lillya, C. P. *J. Am. Chem. Soc.* **1991**, *113*, 8577−8583. (b) Maldivi, P.; Bonnet, L.; Giroud-Godquin, A. M.; Ibn-elhaj, M.; Guillon, D.; Skoulios, A. *Adv. Mater.* **1993**, *5*, 909−912.
(35) Destrade, C.; Gasparoux, H.; Foucher, P.; Tinh, N. H.; Malthête, J.; Jacques, J. *J. Chim. Phys.-Chim. Biol.* **1983**, *80*, 137−148.
(36) Paraschiv, I.; Delforterie, P.; Giesbers, M.; Posthumus, M. A.; Marcelis, A. T. M.; Zuilhof, H.; Sudhölter, E. J. R. *Liq. Cryst.* **2005**, *32*, 977−983.
(37) Imrie, C. T.; Henderson, P. A. *Curr. Opin. Colloid Interface Sci.* **2002**, *7*, 298−311.
(38) Viney, C.; Russell, T. P.; Depero, L. E.; Twieg, R. J. *Mol. Cryst. Liq. Cryst.* **1989**, *168*, 63. Viney, C.; Twieg, R. J.; Russell, T. P.; Depero, L. E. *Liq. Cryst.* **1989**, *5*, 1783.

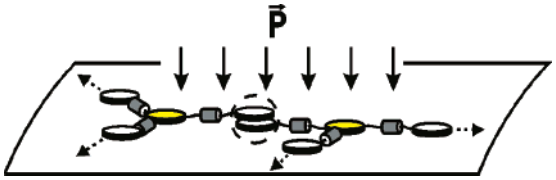

Figure 7. Mechanical alignment of tetramer **16**.

grafting of semifluorinated chains was also found to enhance the structural organization of mesogenic triphenylenes.[20] Even if the chemical incompatibility of alkyl chains with disiloxane is smaller than that with fluorinated chains, examples are known where terminal siloxane groups influenced, via microsegregation, the structural organization of both calamitic[39] and discotic mesogens.[23d]

For none of the other siloxane-containing triphenylenes experimental evidence of such a microsegregation has been found. Microsegregation is extremely efficient in multiblock copolymers, where the entropy of mixing per unit volume is rather small, allowing weak incompatibilities between blocks to provide the energy necessary for segregation. However, for molecular systems, the chemical incompatibility between different portions of the molecule should be strong (polar/nonpolar; hydrophilic/aromatic; lipophilic/fluorophilic) to promote microsegregation; otherwise, the different molecular parts can mix in the mesophase, as has been suggested for the high-temperature mesophase of semifluorinated alkanes.[38] This is probably the case for compounds **3**, **4**, and **5** for which the volume fraction of the siloxane part is small, which is diluted within the aliphatic continuum.

Intracolumnar distances vary from 3.5 up to 3.65 Å for most compounds. Compound **7**, having six pentenyloxy chains, has the largest stacking distances, around 3.65−3.70 Å. The reduced degrees of freedom due to the rigidity of the terminal double bonds and shorter chains may restrict the number of available conformations, increasing the effective contact distance between discogens. A clear increase in $\pi-\pi$ distance is seen on heating, although no quantitative conclusions can be drawn from our experimental data. Compound **8** shows no stacking signal and in the case of compound **14** the signal is so weak that no data could be extracted.

From the width of the $\pi-\pi$ stacking peaks, the intracolumnar correlation length in the mesophase of each compound but **8** and **14** was estimated. The correlation lengths for intracolumnar stacking vary from 50 to 70 Å (that is about 15−20 repeating units) and are very dependent on the temperature, decreasing as the temperature increases, although no precise mathematical relationship between temperature and length can be deduced from our data. In the case of compound **14**, the very weak $\pi-\pi$ stacking signal suggests that either the correlation length is small or that the normal of the cores is slightly tilted with respect to the columnar axis (maybe due to the nonsymmetrical substitution pattern). Hexagonal lattice parameters show little variation with temperature: for instance, compound **9**, possessing the widest mesomorphic temperature range, shows only a 0.1 Å variation between the highest and lowest measured temperatures.

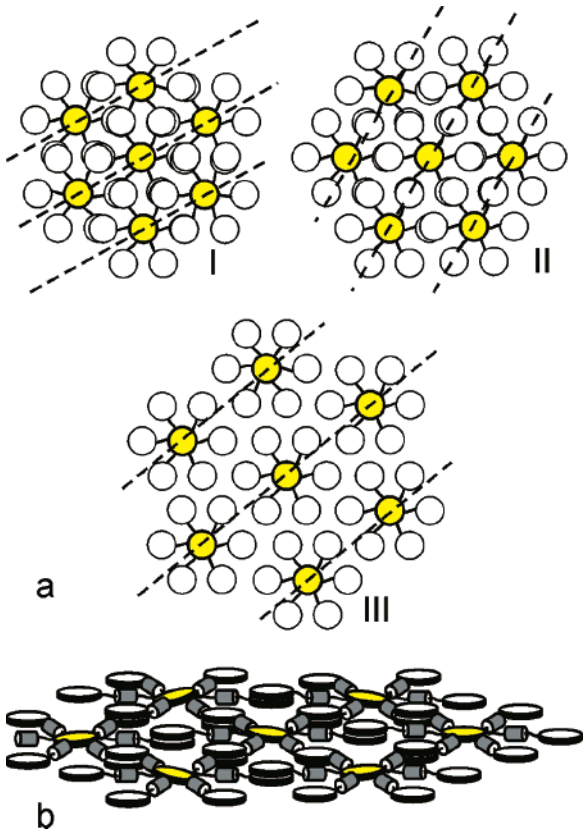

Figure 8. (a) Schematic representation of possible packing modes of the heptamer and (b) packing model for **9** in the Col_h phase. Yellow circles correspond to the central triphenylene bearing six peripheral siloxane fragments, and the white circles correspond to the peripheral triphenylene moieties.

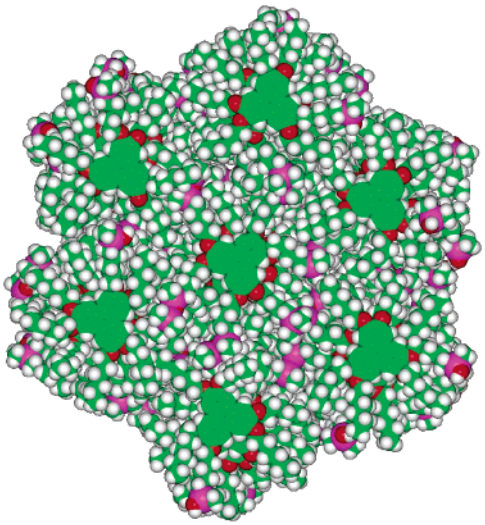

Figure 9. Snapshot of the heptamer **9** in the Col_h phase obtained by MD simulation. Carbon atoms are depicted in green, oxygen atoms in red, silicon atoms in magenta and hydrogen atoms in white.

Oriented XRD patterns of compound **16** confirmed it could be oriented by simply rolling a sample between two glasses. The pattern showed two sets of signals at 19.3 and 3.6 Å, corresponding to the 10 reflections of the hexagonal lattice and to the $\pi-\pi$ stacking (Figure 6). These sets of spots are

(39) (a) Ibn-elhaj, M.; Skoulios, A.; Guillon, D.; Newton, J.; Hodge, P.; Coles, H. J. *Liq. Cryst.* **1995**, *19*, 373. (b) Newton, J.; Coles, H.; Hodge, P.; Hannington, J. *J. Mater. Chem.* **1994**, *4*, 869.

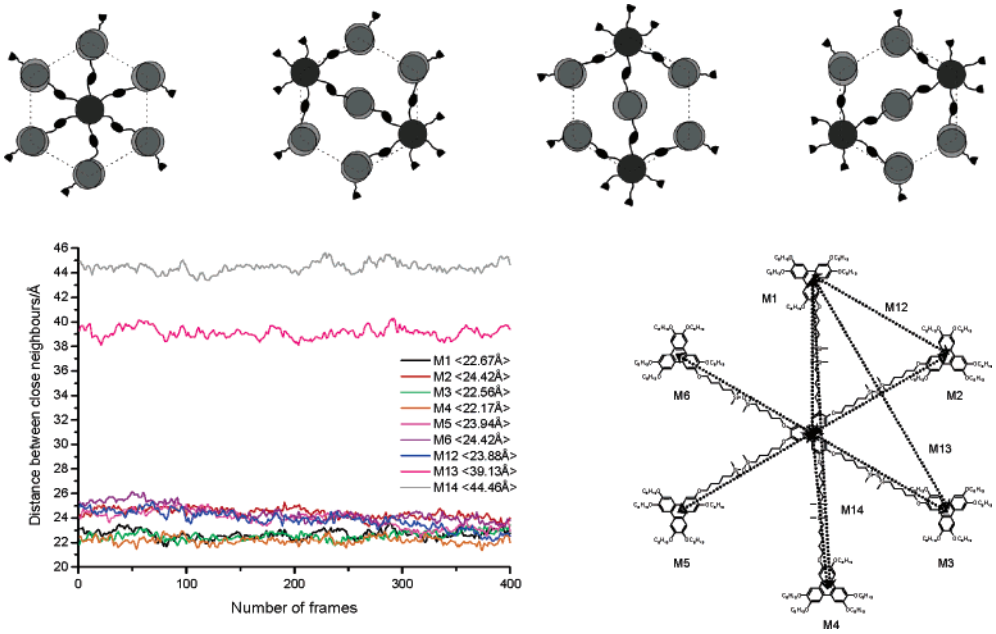

Figure 10. Scheme of the four successive strata used to build the fiber-like molecular model. Each stratum contains a full molecule of heptamer **9** and/or some fraction of it (sectioned at the middle of the siloxane group) to simulate the participation of a neighboring molecule in the stacking of a given rod while sharing one of its side triphenylene moieties. Each triphenylene stack in the resulting cell contains six side groups (drawn in gray) and one central part (drawn in black). Evolution of the intercolumnar distances as a function of time (as given in the molecular scheme) and average distances during the 200 ps simulation.

perpendicular to each other, indicating that the normal of the aromatic cores is perfectly aligned with the columnar axis. The 10 reflection occurred in the plane containing both the incident beam and the cylindrical sample, while the $\pi-\pi$ stacking reflection ocurred in a plane perpendicular to the sample, indicating that the columns, and the normal of the disks, are radially distributed. A plausible mechanism for such a orientation, where the columns lie perpendicular to the cylindrical sample surface, is depicted in Figure 7: the $\pi-\pi$ interactions between triphenylene units of adjacent molecules give cohesion to the system, forming a transient and weak supramolecular polymeric network.[40] The pressure applied when rolling forces the sample to flow in a direction perpendicular to the applied force, stretching the pseudopolymer and thus aligning the sample. This kind of behavior should be observed also in compounds **9** and **17** and maybe even in compound **5**, but their mechanical properties at room temperature made it difficult to process them in the same way: the heat developed by the friction partially melts compound **16** (melting at 30.5 °C) but not the others (melting points ranging between 38 and 54 °C). We are currently exploring new ways of exploiting this elastomer-like behavior.[41]

Heptamer **9** shows the highest clearing temperature and the longest intracolumnar correlation length of all the studied compounds, even if its core is similar to that of **8** which has the lowest clearing temperature. The lack of signal at 6.4 Å in XRD patterns of compound **9** suggests that there is in fact no contact between siloxane chains of different molecules. In addition, a signal at twice the intercolumnar distance shows that there is some structure besides the hexagonal columnar arrangement. When considering the possible packing modes (models **I**, **II**, and **III** in Figure 8a), in which none, one, or two pairs of triphenylene units are interdigitated between each pair of heptamers, the only packing consistent with X-ray experiments is **II** (each heptamer shares one peripheral triphenylene with six adjacent neighbors), where the distance between planes containing the cores is twice that of the regular hexagonal lattice, in agreement with the superstructure. In model **I** (each heptamer shares two peripheral triphenylene with three adjacent neighbors) the interplanar distance is 1.5 times the intercolumnar distance, while in model **III** (the "ideal packing") the hexagonal pattern is scaled up by a factor of $\sqrt{7}$. Within this packing mode, the siloxane density is modulated, leading to different environments for adjacent points in the primitive hexagonal lattice. It should be noted that such a packing prevents the contact between siloxane chains, as shown in Figure 8b. This kind of arrangement is not possible with **8** (and not favored with **14** and **15**) where siloxane interactions are unavoidable.

This higher degree of order (superstructure) has often been found in triphenylene systems. The driving force for the ordering of these systems is always microsegregation due to strong attractive interactions, usually between aromatic parts. Segregation of aromatic substituents,[42] of backbone in side chain polymers,[43] of dendritic core on triphenylene decorated dendrimers,[26a] and of fullerene substituents in triphenylene derivatized fullerenes[44] have been proposed. For star-shaped oligomeric compounds containing six peripheral

(40) Mark, J. E.; Erman, B. In *Rubberlike elasticity*; John Wiley & Sons: New York, 1988; Chapter 3.
(41) Zelcer et al. Work in progress.
(42) Kettner, A.; Wendorff, J. H. *Liq. Cryst.* **1999**, *26*, 483−487.
(43) Ba, C. Y.; Shen, Z. R.; Gu, H. W.; Guo, G. Q.; Xie, P.; Zhang, R. B.; Zhu, C. F.; Wan, L. J.; Li, F. Y.; Huang, C. H. *Liq. Cryst.* **2003**, *30*, 391−397.
(44) Bushby, R. J.; Hamley, I. W.; Liu, Q. Y.; Lozman, O. R.; Lydon, J. E. *J. Mater. Chem.* **2005**, *15*, 4429−4434.

triphenylene units, Ringsdorf and co-workers[16b] did not find any experimental evidence of superstructure; moreover, they concluded that the "ideal stacking" able to produce such superstructure (core over core without the formation of dynamic intermolecular network) is entropically disfavored with respect to the "statistical packing",[16b] a situation that could be modified via specific attractive interactions between cores or between spacers. In the case of compound **9**, and to a lesser extent **16** and **17**, the steric interactions between spacers give rise to the described superstructure, instead of the "ideal stacking" one.

Such a view of the molecular packing of **9** is supported by molecular dynamics simulation (Figure 9). In agreement with the X-ray experimental data, the siloxane fragments are totally "miscible" with the aliphatic fragments, leading to indiscernible triphenylene columns.

This molecular model of single heptamer-based interlocked columns or "fibers" made from seven columns was built according to Figure 10. The model resulted in a quadratic cell of dimension 110 × 110 Å (much larger than the expected diameter of the fiber so that interactions between adjacent fibers can be avoided in the MD simulations) and 25.2 Å in thickness (7 × 3.6 Å, Table 1), corresponding to the height of seven triphenylene cores stacked on top of each other. The model is first minimized in energy to relax some local intermolecular interactions, and a first MD simulation is performed as a 50 ps isotherm at 80 °C. The data for the distance calculations given in the graph of Figure 10 were then collected from a further 200 ps isotherm simulation. It can be clearly seen that the average intercolumnar distances converge toward the measured lattice parameter (Table 1, a = 22.2 Å).

Conclusions

We have developed a new family of hybrid triphenylene-based liquid crystals. The use of a triblock architecture based on triphenylene aromatic cores, alkyl chains, and siloxane segments, together with the typical characteristics of liquid-crystalline oligomers gave rise to improved thermal behavior: lower melting points and glass transition temperatures, higher isotropization points, and little tendency to crystallize. All of the studied compounds showed hexagonal columnar phases, most of them possessing quasi-long-range intracolumnar stacking. The mesophase structure of compound **9** show a superlattice, induced by steric hindrance between siloxane groups.

The thermal behavior of these compounds is strongly dependent on the geometry in the case of the crystalline to columnar transition, but little difference has been found for the columnar to isotropic transition.

The interactions between multiple pairs of oligomers introduce weak network-like properties that, together with the collective behavior characteristic of liquid crystals, can be exploited to align these materials in macroscopic domains.

Although the use of siloxane as dendrimer core[45] or as dimer bridge[46] is common, its use in well-defined oligomers is not usual. Our synthetic strategy, using a silane-mesogen hybrid as a hydrosilylating reagent, allows realizing virtually any siloxane-bridged oligomer, not just with triphenylene, opening the door to many new hybrid siloxane-containing materials.

Experimental Section

Materials. 1,1,1,3,3-Pentamethyldisiloxane (PMDS) (ABCR, Aldrich), 1,1,3,3-tetramethyldisiloxane (TMDS) (ABCR, Aldrich), 5-bromo-pent-1-ene (Aldrich), veratrol (Fluka), and Kardstet's catalyst 2% on xylenes (ABCR) were used as purchased. 2,3,6,7,-10,11-Hexakis(hexyloxy)triphenylene (**HAT6**),[30] 2,3,6,7,10,11-hexamethoxytriphenylene (**HAT1**),[23d,30] 2,3,6,7,10,11-hexahydroxytriphenylene (**6**),[23,31] and 2-hydroxy-3,6,7,10,11-pentakis(hexyloxy)triphenylene (**1**), 2,6,10-tris(hidroxy)-3,7,11-tris(hexyloxy)triphenylene (**11**), and 2,7,11-tris(hidroxy)-3,6,10-tris(hexyloxy)triphenylene (**10**) were synthesized following published procedures[28] with 45%, 29%, and 23% yields, respectively. Thiophene-free toluene was prepared and dried by standard procedures.[47] Only high m/z peaks of intensity superior to 10% of $M^{+\bullet}$ are reported.

Synthetic Methods. *2,3,6,7,10-Pentakis-hexyloxy-11-pent-4-enyloxy-triphenylene (2).* **1** (3.11 g, 4.2 mmol) and 4.8 g of K_2CO_3 were suspended on 100 mL of ethanol. One milliliter (8.4 mmol) of 5-bromo-pent-1-ene was added and the mixture was heated at reflux for 48 h. The solution was poured over HCl (10%) and extracted with CH_2Cl_2 (3 × 60 mL). The organic phase was dried with $MgSO_4$ and evaporated. The solid was purified by flash chromatography on silica gel (hexanes/CH_2Cl_2 1:1) and crystallized from ethanol, yielding 2.95 g (86.8%) of a slightly yellow powder. Analysis: Found (calcd) for $C_{53}H_{80}O_6$ (MW = 813.2): C, 78.21 (78.28); H, 10.01 (9.92). ^{1}H NMR ($CDCl_3$): δ 7.84 (s, 6H), 5.94 (m, 1H), 5.11 (m, 1H), 5.04 (m, 1H), 4.23 (t, 12H), 2.36 (dd, 2H), 2.09−1.90 (m, 12H), 1.58 (m, 10H), 1.35−1.44 (m, 20H), 0.94 (t, 15H).

1,1,3,3,3-Pentamethyl-1-[5-(3,6,7,10,11-pentakis-hexyloxy-triphenylen-2-yloxy-pentyl]-disiloxane (3). A mixture of 0.236 g (0.3 mmol) of **2** and 0.6 mL (0.3 mmol) of PMDS were dissolved on 3 mL of dry toluene. Nine microliters of catalyst was then added and the mixture was heated to 67 °C for 24 h. After removal of the solvent, the product was purified by column chromatography on silica gel (hexanes/CH_2Cl_2 8:2) to yield 0.21 g (75.3%) of a waxy white solid. Analysis: Found (calcd) for $C_{58}H_{96}O_7Si_2$ (MW = 961.55): C, 72.62 (72.45); H, 10.03 (10.06). ^{1}H NMR ($CDCl_3$): δ 7.84 (s, 6H), 4.23 (t, 12H), 1.94 (q, 12H), 1.58 (m, 12H), 1.40 (m, 22H), 0.94 (t, 15H), 0.59 (t, 2H), 0.07 and 0.06 (s, 15H).

1,1,3,3-Tetramethyl-1-[5-(3,6,7,10,11-pentakis-hexyloxy-triphenylen-2-yloxy)-pe ntyl]-disiloxane (4). **2** (2.218 g, 2.7 mmol) and an excess of TMDS (5 mL, 28 mmol) were dissolved in 30 mL of dry toluene. Eight microliters of catalyst was then added and the solution was stirred for 24 h, and 3 mL of TMDS was then added. After another 24 h the solvent and the excess TMDS were evaporated and the product was purified by column chromatography over silica (hexanes/CH_2Cl_2 8:2), yielding 0.958 g (37.1%) of a photosensitive

(45) Lang, H.; Luhmann, B. *Adv. Mater.* **2001**, *13*, 1523−1540.
(46) See for example (a) Guillon, D.; Osipov, M. A.; Mery, S.; Siffert, M.; Nicoud, J. F.; Bourgogne, C.; Sebastiao, P. *J. Mater. Chem.* **2001**, *11*, 2700−2708. (b) Robinson, W. K.; Carboni, C.; Kloess, P.; Perkins, S. P.; Coles, H. J. *Liq. Cryst.* **1998**, *25*, 301−307.
(47) Perrin, D. D.; Aramego, W. L. F. *Purification of Laboratory Chemicals*; Butterworth-Heinemann: Oxford, 1996.

white product. Analysis: Found (calcd) for $C_{57}H_{94}O_7Si_2$ (MW = 946.65): C, 71.92 (72.25); H, 9.91 (10.00). ^{1}H NMR ($CDCl_3$): δ 7.84 (s, 6H), 4.69 (m, 1H), 4.23 (t, 12H), 1.94 (q, 12H), 1.58 (m, 12H), 1.40 (m, 22H), 0.93 (t, 15H), 0.61 (t, 2H), 0.17 (d, 6H), 0.08 (s, 6H). MS (EI): *m*/*z* 862.5 (15%), 946.6 (100%, $[M]^{+\bullet}$), 1020.6 (14%, $[M + Si(CH_3)_2O]^{+\bullet}$), 1808.1 (19%), 1893.1 (33%, $[2M]^{+\bullet}$), 1967.1 (12%, $[2M + Si(CH_3)_2O]^{+\bullet}$). MS (MALDI-TOF): 946.65 ($[M]^{+\bullet}$), 947.65 ($[M + 1]^{+\bullet}$), 948.67 ($[M + 2]^{+\bullet}$), 1020.67 ($[M + Si(CH_3)_2O]^{+\bullet}$), 1021.67 ($[M + 1 + Si(CH_3)_2O]^{+\bullet}$), 1022.68 ($[M + 2 + Si(CH_3)_2O]^{+\bullet}$).

*1,1,3,3-Tetramethyl-1,3-bis-[5-(3,6,7,10,11-pentakis-hexyloxy-triphenylen-2-ylo xy)-pentyl]-disiloxane (**5**).* Four microliters of catalyst was added to a solution of 520 mg (0.64 mmol) of **2** and 50 μL of TMDS in 20 mL of toluene. The solution was heated to 45 °C for 20 h when ^{1}H NMR indicated incomplete reaction, probably owing to the high volatility of TMDS. Yet another 50 μL of TMDS and 5 μL of catalyst were then added and the reaction was kept at 45 °C for another 24 h. The solvent was evaporated and the solids were purified by column chromatography on silica gel (hexanes/CH_2Cl_2), yielding 204 mg (36%) of a slightly pink powder. Analysis: Found (calcd) for $C_{110}H_{174}O_{13}Si_2$ (MW = 1760.72): C, 74.54 (75.04); H, 9.93 (9.96). ^{1}H NMR ($CDCl_3$): δ 7.82 (s, 12H), 4.22 (t, 24H), 1.93 (q, 24H), 1.57 (m, 24H), 1.34−1.44 (m, 44H), 0.93 (t, 30H), 0.59 (t, 4H), 0.07 (s, 12H). ^{13}C NMR ($CDCl_3$): δ 148.98, 123.62, 107.40, 69.72, 31.68, 29.90, 29.68, 29.44, 25.84, 23.27, 22.65, 18.43, 14.03, 0.38.

*2,3,6,7,10,11-Hexakis-pent-4-enyloxy-triphenylene (**7**).* 2,3,6,7,-10,11-Hexahydroxytriphenylene **6** (3.376 g, 10.4 mmol) and 18.42 g of K_2CO_3 were suspended in 230 mL of ethanol and the solution was degassed applying three cycles of vacuum/argon. Nine milliliters (75.6 mmol) of 5-bromo-pent-1-ene were then added and the mixture was refluxed for 24 h. After cooling, the mixture was poured over CH_2Cl_2, filtered to remove excess K_2CO_3, and evaporated. The residue thus obtained was purified by column chromatography over silica (AcOEt/hexanes 3:100), yielding 2.506 g (32.9%) of a slightly pink powder. Analysis: Found (calcd) for $C_{48}H_{60}O_6$ (MW = 732.99): C, 78.16 (78.65); H, 8.25 (8.25). ^{1}H NMR ($CDCl_3$): δ 7.83 (s, 6H), 5.94 (m, 6H), 5.12 (m, 6H), 5.04 (m, 6H), 4.25 (t, 12H), 2.37 (m, 12H), 2.05 (q, 12H). ^{13}C NMR ($CDCl_3$): δ 148.89, 137.92, 123.62, 115.16, 107.43, 68.87, 30.24, 28.63.

*2,3,6,7,10,11-Hexakis-[5-(1,1,3,3,3-pentamethyl-disiloxanyl)-pentyloxy]tripheny lene (**8**).* **7** (0.2 g, 0.27 mmol) and 0.74 g (5 mmol) of PMDS were dissolved in 3 mL of dry toluene. Five microliters of catalyst was added and the solution was heated to 60 °C for 24 h, when 4 μL of catalyst was added. Twenty-four hours later, the solvent was removed and the pasty material was chromatographed on silica using hexanes/CH_2Cl_2 (9:1) as a solvent, yielding 0.260 g (58.7%) of a transparent material. Analysis: Found (calcd) for $C_{78}H_{156}O_{12}Si_{12}$ (MW = 1623.09): C, 57.74 (57.72); H, 9.71 (9.69). ^{1}H NMR ($CDCl_3$): δ 7.85 (s, 6H), 4.21 (t, 12H), 1.96 (dd, 12H), 1.65−1.43 (24H), 0.6 (t, 12H), 0.07 and 0.06 (90H). ^{13}C NMR ($CDCl_3$): δ 148.96, 123.61, 107.43, 69.68, 29.79, 29.23, 23.18, 18.34, 1.94, 0.32. MS (FAB): 1620.65 ($[M]^{+\bullet}$), 1621.65 ($[M + 1]^{+\bullet}$), 1622.65 ($[M + 2]^{+\bullet}$), 1623.65 ($[M + 3]^{+\bullet}$), 1624.65 ($[M + 4]^{+\bullet}$), 1625.70 ($[M + 5]^{+\bullet}$), 1626.70 ($[M + 6]^{+\bullet}$).

*Star-like Heptamer (**9**).* Sixty milligrams (82 μmol) of **7** and 0.776 g (819 μmol) of **4** were dissolved in 10 mL of dry toluene, and 18 μL of catalyst was added. The solution was stirred for 48 h, the solvent evaporated, and the product purified by column chromatography (hexanes, CH_2Cl_2 3:1 up to 1:1), yielding 0.327 g (62.2%) of a sticky compound. Analysis: Found (calcd) for $C_{390}H_{624}O_{48}Si_{12}$ (MW = 6418.12): C, 72.95 (72.98); H, 9.76 (9.80). ^{1}H NMR ($CDCl_3$): δ 7.81 and 7.79 (s, 42H), 4.21 (m, 84H), 1.92 (m, 84H), 1.57 (m, 84H), 1.39 (m, 144H), 0.93 (m, 90H), 0.59 (t, 24H), 0.07 (s, 72H). ^{13}C NMR ($CDCl_3$): δ 149.02, 123.66, 107.48, 69.76, 31.69, 29.94, 29.46, 29.36, 25.87, 23.305, 22.65, 18.457, 14.03, 0.42, 0.02. MS (MALDI-TOF): *m*/*z* 6418.2 ($[M]^{+\bullet}$), 6493.2 ($[M + Si(CH_3)_2O]^{+\bullet}$), 6586.8 ($M + 2{\cdot}Si(CH_3)_2O]^{+\bullet}$). Polydispersity (GPC): 1.07.

*2,6,11-Tris(hexyloxy)-3,7,10-tris(pent-4-enyloxy)-triphenylene (**12**).* Phenol **10** (1.384 g, 2.4 mmol) and 2 g of K_2CO_3 were suspended in 50 mL of DMF under an argon atmosphere. Then 1.1 mL (9.3 mmol) of 5-bromo-pent-1-ene was added and the solution was heated to 80 °C for 24 h when TLC showed complete reaction. Two hundred milliliters of CH_2Cl_2 was then added and excess K_2CO_3 was filtered. Solvents were evaporated, the yellowish compound was dissolved in CH_2Cl_2 and washed with diluted HCl and then with water. The organic phase was dried ($MgSO_4$) and evaporated. The solid thus obtained was crystallized from ethanol and then from isopropanol, yielding 1.1317 g (60.4%) of white needles. Analysis: Found (calcd) for $C_{51}H_{72}O_6$ (MW = 781.11): C, 77.94 (78.42); H, 9.27 (9.29). ^{1}H NMR ($CDCl_3$): δ 7.84 (6H), 5.94 (m, 3H), 5.11 (m, 3H), 5.04 (m, 3H), 4.25 (m, 3H), 2.37 (m, 6H), 2.09−1.90 (m, 12H), 1.58 (6H), 1.44−1.35 (m, 12H), 0.94 (t, 9H). ^{13}C NMR ($CDCl_3$): δ 149.00, 148.85, 137.96, 123.66, 123.55, 115.10, 107.3, 69.65, 68.94, 31.63, 60.22, 29.38, 28.63, 25.82, 22.61, 14.00.

*2,6,10-Tris(hexyloxy)-3,7,11-tris(pent-4-enyloxy)-triphenylene (**13**).* In a similar way, 1.115 g (1.9mmol) of **11** and 2 g of K_2CO_3 were suspended in 50 mL of DMF and 1.1 mL (9.3mmol) of 5-bromo-pent-1-ene was added. The solution was kept at 80 °C for 24 h, 200 mL of CH_2Cl_2 was added, and the excess K_2CO_3 was filtered. The solvents were evaporated and the crude sample was chromatographed on silica (hexanes/CH_2Cl_2 8:2 up to 2:1) and crystallized from ethanol, yielding 0.818 g (54.2%) of a white powder. Analysis: Found (calcd) for $C_{51}H_{72}O_6$ (MW = 781.11): C, 78.15 (78.42); H, 9.36 (9.29). ^{1}H NMR ($CDCl_3$): δ 7.85 and 7.84 (6H), 5.94 (m, 3H), 5.11 (m, 3H), 5.04 (m, 3H), 4.25 (m, 12H), 2.37 (m, 6H), 2.09−1.90 (m, 12H), 1.58 (m, 12H), 1.44−1.35 (m, 12H), 0.93 (t, 9H).

*2,6,11-Tris(hexyloxy)-3,7,10-tris-[5-(1,1,3,3,3-pentamethyl-disiloxanyl)-pentyloxy]-triphenylene (**14**).* Alkene **12** (0.412 g, 527 μmol) and 0.357 g (2.4 mmol) of PMDS were dissolved in 3 mL of dry toluene. Seven microliters of catalyst was added and the solution was kept stirring at room temperature for 48 h. Solvent was evaporated and the crude product was purified by chromatography (silica, cyclohexane/CH_2Cl_2 2:1), then dissolved in THF, and precipitated in methanol. Then 0.344 g (53.2%) of a sticky semitransparent material was obtained. Analysis: Found (calcd) for $C_{66}H_{120}O_9Si_6$ (MW = 1226.17): C, 64.61 (64.65); H, 9.99 (9.86). ^{1}H NMR ($CDCl_3$): δ 7.84 (6H), 4.22 (m, 12H), 1.94 (m, 12H), 1.65−1.35 (m, 30H), 0.94 (t, 9H), 0.59 (t, 6H), 0.07 and 0.06 (45H). ^{13}C NMR ($CDCl_3$): δ 148.99, 123.63, 107.41, 69.74, 69.70, 31.69, 29.85, 29.43, 29.29, 25.84, 23.22, 22.66, 18.36, 14.04, 1.97, 0.34. MS (MALDI-TOF): *m*/*z* 1224.7 ($[M]^{+\bullet}$), 1225.7 ($[M + 1]^{+\bullet}$), 1226.7 ($[M + 2]^{+\bullet}$), 1227.7 ($[M + 3]^{+\bullet}$), 1228.7 ($[M + 4]^{+\bullet}$), 1229.7 ($[M + 5]^{+\bullet}$), 1230.7 ($[M + 6]^{+\bullet}$).

*2,6,10-Tris(hexyloxy)-3,7,11-tris-[5-(1,1,3,3,3-pentamethyl-disiloxanyl)-pentyloxy]-triphenylene (**15**).* Alkene **13** (0.472 g, 603 μmol) and 0.360 g (2.4 mmol) of PMDS were dissolved in 3 mL of dry toluene. Eight microliters of catalyst was added and the solution was kept stirring at room temperature for 48 h. Solvent was evaporated and the crude product was purified by chromatography (silica, cyclohexane/CH_2Cl_2 2:1), dissolved in THF, and precipitated in methanol. Then 0.201 g (40.6%) of a waxy white material was obtained. Analysis: Found (calcd) for $C_{66}H_{120}O_9Si_6$ (MW = 1226.17): C, 64.87 (64.65); H, 10.09 (9.86). ^{1}H NMR

($CDCl_3$): δ 7.85 (6H), 4.24 (m, 12H), 1.95 (m, 12H), 1.65−1.35 (m, 30H), 0.94 (t, 9H), 0.60 (t, 6H), 0.08 and 0.07 (45H). ^{13}C NMR ($CDCl_3$): δ 149.02, 148.97, 123.62, 107.44, 107.37, 69.76, 69.68, 31.69, 29.86, 29.43, 29.27, 25.86, 23.22, 22.67, 18.39, 14.06, 1.97, 0.34. MS (MALDI-TOF): 1224.7 ($[M]^{+\bullet}$), 1225.7 ($[M + 1]^{+\bullet}$), 1226.7 ($[M + 2]^{+\bullet}$), 1227.7 ($[M + 3]^{+\bullet}$), 1228.7 ($[M + 4]^{+\bullet}$), 1229.7 ($[M + 5]^{+\bullet}$), 1230.7 ($[M + 6]^{+\bullet}$).

*Unsymmetrical Tetramer (**16**).* Alkene **12** (117 mg, 149 μmol) and 681 mg (718 μmol) of silane **4** were dissolved in 5 mL of dry toluene. Eight microliters of catalyst was added and the mixture was stirred for 48 h. The solvent was evaporated and the crude sample was chromatographed on silica (cyclohexane/CH_2Cl_2 3:1 up to 1:1). Then 427 mg (78.7%) of a waxy white compound was obtained. Analysis: Found (calcd) for $C_{222}H_{354}O_{27}Si_6$ (MW = 3623.68): C, 73.15 (73.58); H, 10.03 (9.85). ^{1}H NMR ($CDCl_3$): δ 7.82 and 7.80 (24H), 4.22 (m 48H), 1.93 (m, 48H), 1.57 (m, 48H), 1.40 (m, 84H), 0.93 (t, 54H), 0.59 (t, 12H), 0.06 (36H). ^{13}C NMR ($CDCl_3$): δ 148.96, 123.60, 107.34, 69.70, 31.68, 29.91, 29.43, 29.36, 25.85, 23.28, 22.66, 18.43, 14.04, 0.38. MS (MALDI-TOF): *m/z* 3620.5 ($[M]^{+\bullet}$), 3621.5 ($[M + 1]^{+\bullet}$), 3622.4 ($[M + 2]^{+\bullet}$), 3623.5 ($[M + 3]^{+\bullet}$), 3624.4 ($[M + 4]^{+\bullet}$), 3625.5 ($[M + 5]^{+\bullet}$), 3626.5 ($[M + 6]^{+\bullet}$).

*Symmetrical Tetramer (**17**).* Alkene **13** (121 mg, 155 μmol) and 680 mg (717 μmol) of silane **4** were dissolved in 5 mL of dry toluene. Eight microliters of catalyst was added and the mixture was stirred for 24 h. The solvent was evaporated and the crude sample was chromatographed on silica (cyclohexane/CH_2Cl_2 3:1 up to 1:1). A slightly yellowish compound was obtained, which was dissolved in THF (2 mL), precipitated by dropping on cold methanol, and filtered, yielding 380 mg (67.7%) of a white product. Analysis: Found (calcd) for $C_{222}H_{354}O_{27}Si_6$ (MW = 3623.68): C, 73.50 (73.58); H, 9.96 (9.85). ^{1}H NMR ($CDCl_3$): δ 7.82 and 7.80 (24H), 4.22 (m, 48H), 1.93 (m, 48H), 1.56 (m, 48H), 1.40 (m, 84H), 0.93 (t, 54H), 0.60 (t, 12H), 0.07 (36H). ^{13}C NMR ($CDCl_3$): δ 148.97, 123.60, 107.37, 69.71, 31.68, 29.91, 29.43, 19.31, 25.84, 23.28, 22.66, 18.44, 14.04, 0.38. MS (MALDI-TOF): *m/z* 3620.5 ($[M]^{+\bullet}$), 3621.5 ($[M + 1]^{+\bullet}$), 3622.4 ($[M + 2]^{+\bullet}$), 3623.5 ($[M + 3]^{+\bullet}$), 3624.4 ($[M + 4]^{+\bullet}$), 3625.5 ($[M + 5]^{+\bullet}$), 3626.5 ($[M + 6]^{+\bullet}$).

Characterization Methods. GPC, mass spectra, and elemental analyses were carried out by the service of Charles Sadron Institute, Strasbourg, France. ^{1}H NMR and ^{13}C NMR spectra were measured either on a Bruker Avance300 or a Bruker AM500 spectrometer, using $CDCl_3$ as solvent and its residual peak as internal reference (7.26 ppm for ^{1}H and 77.00 ppm for ^{13}C).

Physicochemical Measurements. Polarized-light optical microscopy observations (POM) as a function of temperature were carried out between cross polarizers on either a Leitz DMRX microscope equipped with a Leitz 1350 hot-stage device (Inquimae) or an Orthoplan (Leitz) microscope (GMO) working in the transmission mode and associated with a Mettler FP82 hot stage and FP80 central processor. Transition temperatures and enthalpies were obtained by DSC experiments at a heating rate of 1, 2, or 5 °C/min alternatively on a Shimadzu DSC-50 (Inquimae), a Perkin-Elmer DSC-7 instrument, or a TA DSCQ1000 (GMO). The XRD patterns were obtained at GMO with two different experimental setups, the powder being filled in Lindemann capillaries of 1 or 0.5 mm diameter and 10 μm thick walls. A linear monochromatic Cu $K\alpha_1$ beam (λ = 1.5418 Å) was obtained using a Guinier camera (900 W) or a Debye−Scherrer camera, both equipped with a bent quartz monochromator and an electric oven. A first set of diffraction patterns was registered with a gas curved counter "Inel CPS 120"; periodicities up to 60 Å could be measured, and the sample temperature was controlled within ±0.05 °C. The second set of diffraction patterns was registered on image plates; periodicities up to 90 Å could be measured, and the sample temperature was controlled within ±0.3 °C. Exposure times were varied from 1 to 30 h. The XRD patterns were carried out from room temperature to 10 °C above the isotropization temperature determined by DSC and POM.

Modeling. The molecular modeling studies were performed on SGI Origin 2800 and Octane^2 calculators using Insight II and Discover 3 software from Accelrys (www.accelrys.com) with the cvff force field. Energy minimization of the model in the fixed cell was conducted down to a gradient of 1 kcal/mol, and the packing was then equilibrated at 373 K by a 50 ps isothermal MD simulation (NVT-PBC ensemble, "velocity scaling" temperature control method, and a time step of 1 fs). The data collection for the distances measurements was done in another MD simulation of a 373 K isotherm (same conditions but with the Andersen temperature control method).

Acknowledgment. We wish to thank Dr. Benoît Heinrich and Mrs. Laurence Oswald (GMO-IPCMS) for invaluable assistance and Dr. Stephane Méry (GMO-IPCMS) for helpful discussions. Financial support from the Fundación Antorchas, UBACyT (X219), and Ecos-Setcip (Grant A01E05 for international cooperation) is acknowledged. A.Z. thanks CONICET for an international doctoral fellowship. F.D.C. is a member of the scientific staff of CONICET. B.D. and D.G. thank the CNRS and the Université Louis Pasteur (Strasbourg).

Supporting Information Available: ^{1}H and ^{13}C NMR spectra, MALDI-TOF, and GPC of selected compound (PDF). This material is available free of charge via the Internet at http://pubs.acs.org.

CM062949B